Cell. Mol. Life Sci. (2014) 71:1927–1941
DOI 10.1007/s00018-013-1451-9

Cellular and Molecular Life Sciences

RESEARCH ARTICLE

Sequential inactivation of Rho GTPases and Lim kinase by *Pseudomonas aeruginosa* toxins ExoS and ExoT leads to endothelial monolayer breakdown

P. Huber · S. Bouillot · S. Elsen · I. Attrée

Received: 8 April 2013 / Revised: 12 July 2013 / Accepted: 5 August 2013 / Published online: 22 August 2013

Abstract *Pseudomonas aeruginosa* is a major human opportunistic pathogen and one of the most important causal agents of bacteremia. For non-blood-borne infection, bacterial dissemination requires the crossing of the vascular endothelium, the main barrier between blood and the surrounding tissues. Here, we investigated the effects of *P. aeruginosa* type 3 secretion effectors, namely ExoS, ExoT, and ExoY, on regulators of actin cytoskeleton dynamics in primary endothelial cells. ExoS and ExoT similarly affected the Lim kinase-cofilin pathway, thereby promoting actin filament severing. Cofilin activation was also observed in a mouse model of *P. aeruginosa*-induced acute pneumonia. Rho, Rac, and Cdc42 GTPases were sequentially inactivated, leading to inhibition of membrane ruffling, filopodia, and stress fiber collapse, and focal adhesion disruption. At the end of the process, ExoS and ExoT produced a dramatic retraction in all primary endothelial cell types tested and thus a rupture of the endothelial monolayer. ExoY alone had no effect in this context. Cell retraction could be counteracted by overexpression of actin cytoskeleton regulators. In addition, our data suggest that moesin is neither a direct exotoxin target nor an important player in this process. We conclude that any action leading to inhibition of actin filament breakdown will improve the barrier function of the endothelium during *P. aeruginosa* infection.

Keywords Host–pathogen interaction · Nosocomial infection · Actin · Signaling pathways · Rho GTPases · Endothelium

Electronic supplementary material The online version of this article (doi:10.1007/s00018-013-1451-9) contains supplementary material, which is available to authorized users.

P. Huber (✉) · S. Bouillot · S. Elsen · I. Attrée
INSERM, U1036, Biology of Cancer and Infection, Grenoble, France
e-mail: phuber@cea.fr

P. Huber · S. Bouillot · S. Elsen · I. Attrée
CNRS, ERL 5261, Bacterial Pathogenesis and Cellular Responses, Grenoble, France

P. Huber · S. Bouillot · S. Elsen · I. Attrée
Université Joseph Fourier-Grenoble I, Grenoble, France

P. Huber · S. Bouillot · S. Elsen · I. Attrée
CEA, DSV/iRTSV, Grenoble, France

Introduction

Pseudomonas aeruginosa is a major cause of nosocomial infections in humans, and clinical isolates are often multiresistant to antibiotics. Like many Gram-negative bacteria, *P. aeruginosa* possesses a type III secretion system (T3SS), constituted of an inject some, through which the bacterium injects exotoxin exhibiting various biological activities directly into target cell cytoplasm [1–3]. T3S effectors are required during acute infection for bacterium transmigration through the epithelial and endothelial barriers [4]. The T3SS is also required for *P. aeruginosa* survival in the blood [4].

Four T3S toxins have been identified: ExoS, ExoT, ExoY, and ExoU. However, few strains isolated so far encode all four toxins and the presence of ExoS and ExoU seem to be mutually exclusive [1–3]. Toxin injection triggers the breakdown of epithelial barriers by altering several host signaling proteins. ExoS and ExoT are 75 % identical at the amino-acid level and have both a GTPase-activating protein (GAP) and an ADP ribosyl transferase (ADPRT) activity. The GAP domains of these toxins are sufficient

to inactivate the Rho family GTPases including RhoA, Rac1, and Cdc42, and to disrupt the cytoskeleton of epithelial cells [5–8]. Identified targets of ExoS ADPRT activity are members of Ras and Rab family GTPases, as well as ezrin/radixin/moesin (ERM) proteins Rac1, Cdc42, and vimentin [9–18]. ADP-ribosylation of two substrates, Ras and moesin, was shown to be particularly important for ExoS-mediated cell intoxication. Overexpression of the active forms of Ras or moesin prevented ExoS-induced cytotoxicity and cell rounding, respectively [19, 20]. ExoT ADPRT activity seems to be restricted to two isoforms of the CT10 regulator of kinase, Crk1, and Crk2, which are adaptor proteins capable of recruiting and assembling protein complexes at focal adhesion (FA) sites, as well as phosphoglycerate kinase-1 [21, 22]. Crk inactivation by ExoT affects several downstream signaling pathways by interfering with focal adhesion-dependent Rac activation [23].

ExoU is a potent phospholipase that induces rapid necrotic cell death by disruption of plasma membrane integrity, while ExoY is an adenylate cyclase with weak toxic activity [24–28].

It is proposed that the final effect of the T3S effectors is to disrupt the tissue barriers in order to permit bacteria dissemination. Studies on ExoS, ExoT, and ExoY pathogenic activities have concentrated on epithelial or myeloid cells, while very few studies report on the infection of the vascular endothelium, the main barrier between the blood and the surrounding tissues. Induction of vascular lesions has nevertheless been recognized as an important parameter in the pathogenesis of *P. aeruginosa*-induced pneumonia [29–31] and crossing of the vascular barrier is a necessary step for bacterial dissemination in non-blood-borne infections.

Pittet's group showed that ExoS and ExoT were responsible for increases in protein permeability across the lung endothelium. Furthermore, they found that Rac1 was inhibited whereas RhoA was activated, which in turn induced the formation of actin stress fibers. This resulted in cell retraction via actomyosin contraction, thereby increasing paracellular permeability [32]. Surprisingly, ExoU had limited effects on endothelial paracellular permeability compared to ExoS and ExoT, while it is recognized as the most potent toxin regarding epithelial barrier disruption. ExoY toxic activity in endothelial cells is controversial since one group reported that ExoY, in absence of other T3S toxins, generated increased endothelial permeability [33], whereas this effect was not found by others [32].

Here, we first examined the activity of T3S effectors in various endothelial cell types and we observed a prominent cell retraction in primary endothelial cells derived from veins, capillaries, and arteries, a feature associated with disruption of the actin cytoskeleton and focal adhesions. This effect was elicited by ExoS and ExoT, but not by ExoY. To investigate the sequence of events leading to endothelial monolayer breakdown, we examined the actin filament dynamics by videomicroscopy and the activities of various signaling proteins in the course of infection of primary endothelial cells. We observed that cell retraction occurred only after total collapse of the actin cytoskeleton, indicating that retraction was not caused by actomyosin contraction. Notably, we show that ExoS and ExoT-induced inactivation of all three Rho GTPases leads to dephosphorylation of Lim kinase, thus inducing the actin filament severing activity of cofilin. In all of these features, ExoS exhibited a much more drastic activity than ExoT. Overexpression of the constitutively active forms of either Rac1, RhoA, Lim kinase, or the form in mDia2 reduced *P. aeruginosa*-induced cell retraction. Finally, lungs from mice with *P. aeruginosa*-induced acute pneumonia exhibited cofilin activation. Altogether, our data suggest that any action preventing actin filament collapse by inhibiting actin filament severing will limit endothelial cell retraction and bacterial dissemination.

Experimental procedures

Bacterial strains

The *P. aeruginosa* strains used in this study are described in Online Resources 1–3.

cAMP dosage

At 4-h post-infection, HUVECs were extensively washed with PBS and lysed in 0.1 M HCl. Supernatants were collected and assayed for cAMP content by using the cAMP ELISA kit from Enzo.

Immunofluorescence staining and cell retraction assay

For myc, paxillin, and F-actin staining, cells were fixed with 4 % paraformaldehyde for 15 min and permeabilized by 0.5 % triton X-100 for 5 min. For microtubule staining, cells were first treated for 2 min with cold OPT buffer (80 mM Pipes pH 6.7, 1 mM EGTA, 1 mM $MgCl_2$, 0.5 % Triton, 10 % glycerol) to lyse cells and dilute free tubulin. Cells were then stained using standard procedure with appropriate primary and secondary antibodies or phalloidin-FITC. Stained cells were observed with a Zeiss epifluorescence microscope (Axioplan).

For the cell retraction assay, cells were fixed in methanol at −20 °C for 10 min and labeled for actin and with Hoechst for cell count. Images were captured with a low-magnification objective (16×) and treated with ImageJ software. Briefly, images of actin staining were binarized and

the total cell surface was calculated for each image. Cell number was in the range of 570–640 per image in the non-infected conditions. This number decreased to 400–420 post-*Pa*-S infection.

For transfection of the active forms of RhoA, Rac1, Lim kinase, and mDia2, the assay described above could not be used because all cells were not transfected. Therefore, retraction cells were scored individually after selection of transfected cells either by GFP expression (RhoA, Rac1, mDia2) or after myc labeling (Lim kinase). Tresholding was performed by ImageJ software. Retracted cells were scored by the experimenter after actin labeling. The total number of counted cells for each condition is indicated in Fig. 9.

Rho GTPase activity assay

Rho, Rac, and Cdc42 activation assays were performed in triplicate using G-LISA kits from Cytoskeleton.

Transendothelial albumin flux

Measurement was done using established procedures. Briefly, HUVECs were seeded onto tissue culture inserts containing porous membranes (Greiner). Once confluent, cells were infected as described above by addition of bacteria in the upper compartment. Five micrograms of bovine serum albumin coupled to TRITC (Nordic Immunological) were simultaneously added to the upper compartment. Fluorescence in the lower compartment was measured at 4.5 h p.i. in a fluorescence plate reader (Thermo Scientific).

Animals

All protocols in this study were conducted in strict accordance with the French guidelines for the care and use of laboratory animals. The protocol for mouse infection was approved by the animal research committee of the institute (CETEA). Pathogen-free Balbc male mice (8–10 weeks) were obtained from Harlan Laboratories and housed in the CEA animal care facility.

P. aeruginosa-induced lung injury

Bacteria in exponential growth were prepared as indicated above, centrifuged, and resuspended in sterile PBS at $1.7.10^8$/ml as evaluated by spectroscopy. Mice were anesthetized by intraperitoneal administration of a mixture of xylazine (10 mg/kg) and ketamine (50 mg/kg). Then, 30 µl of bacterial suspension (i.e., 5.10^6 bacteria) were deposited into mouse nostrils. Mice were euthanized by CO_2 inhalation 16 h later. Lungs were resected and lysed for protein extraction. Full methods are available in Online Resource 2.

Results

ExoS and ExoT, but not ExoY induce endothelial cell retraction

P. aeruginosa T3SS induces actin cytoskeleton collapse and cell retraction in several cell types [34]. Here we investigated the effect of *P. aeruginosa* on several endothelial cell types by using the wild-type PAO1F strain and observed cell behavior by microscopy. For infection, cells in confluent monolayers were incubated and infected in the same culture medium to prevent *P. aeruginosa* growth variations. At 3-h post-infection at MOI 10, cells were simultaneously fixed and labeled with anti-actin antibody to stain the entire cell body (Online Resource 4). Human umbilical cord endothelial cells (HUVEC), human microvascular lung endothelial cells (HMVEC) and bovine aortic endothelial cells (BAEC) all showed extensive retraction. Thus, endothelial cells from venous, microvascular, or arterial vessels are all sensitive to *P. aeruginosa* to a similar extent. In contrast, infection of mouse endothelioma cells (H5 V) and rat brain endothelial cells (RBE4) exhibited little or no retraction. This difference may be due to the transformed nature of the latter cell lines as opposed to the primary culture of the former cells. Alternatively, *P. aeruginosa* toxicity may be less efficient in rodent cells, although rats and mice are routinely used as infection models for this pathogen. In comparison, the human carcinoma cell line A549 showed extensive cell rounding and cell–cell contact loss, but retraction was not as extensive as in primary endothelial cells.

To precisely determine the cell retraction capacity of *P. aeruginosa* mutants affected in their T3SS composition (Online Resource 1), retraction was quantified in HUVECs after fixation and actin labeling (Fig. 1a, b). A mutant strain deleted for ExoS, ExoT and ExoY (Δ*3Tox*; Fig. 1b) did not significantly affect total cell surface, indicating that cell retraction was caused by T3SS exotoxins. The double-deletion mutants ΔExoT–ΔExoY and ΔExoS–ΔExoY, injecting only ExoS (*Pa*-S) or ExoT (*Pa*-T), respectively, also induced cell retraction, which was even more striking than the wild-type in the case of *Pa*-S ($p = 0.006$). Indeed, quantification of cell retraction shows that *Pa*-S was more toxic than *Pa*-T. To further establish *Pa*-induced cell retraction by ExoS and ExoT, we analyzed endothelial cell monolayer integrity in a permeability assay using albumin-TRITC as a tracer (Online Resource 5). *Pa*-WT, *Pa*-S, and *Pa*-T all induced a similar increase in paracellular albumin flux compared to the non-infected monolayer. Interestingly, the Δ*3Tox* mutant induced a smaller but significant increase in albumin flux indicating that *Pa*-secreted factors other than the T3SS may alter endothelial integrity.

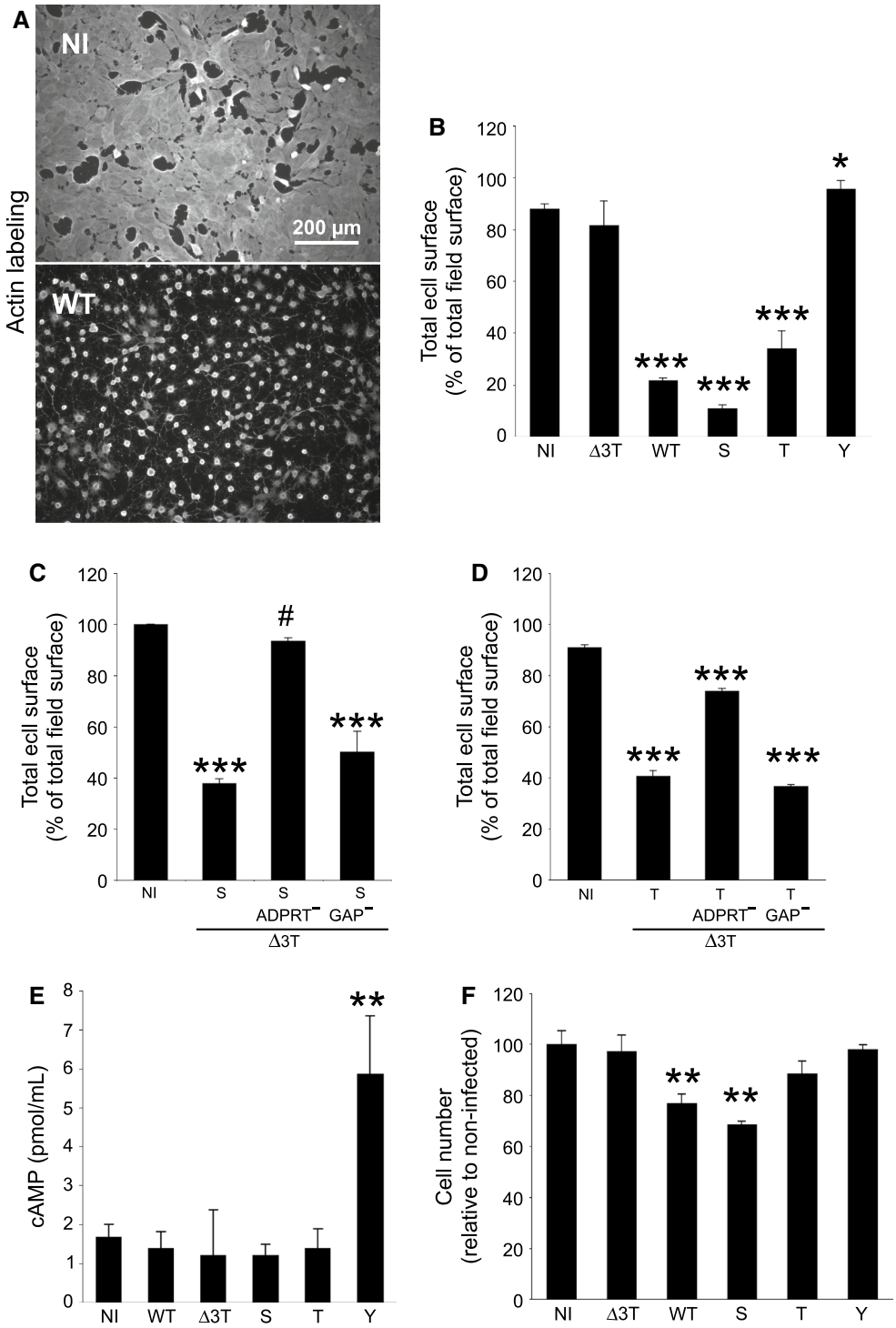

Fig. 1 Analysis of cell retraction and detachment induced by T3SS mutants. **a–d** HUVECs were infected *Pa* mutants for 4 h, then fixed and labeled with anti-β-actin antibodies. **a** Three fluorescent images were captured for each condition at low magnification field and the total surface occupied by the cells was calculated for each image. **b** The results are presented as the average percentage (+SD) of total cell surface over image surface. The histograms represent total cell surface in absence of infection (NI), or when infected with *Pa*-Δ3Tox (Δ3T), *Pa*-WT (WT), *Pa*-S (S), *Pa*-T (T), or *Pa*-Y (Y). **c** Analysis of cell retraction induced by *P. aeruginosa* expressing ExoS (S), or ExoS activity domain mutants $ExoS_{ADPRT^-}$ and $ExoS_{GAP^-}$ in *Pa*-Δ*3Tox* background. **d** Similar analysis with activity domain mutants of ExoT. **e** cAMP levels in HUVECs were measured at 4 h p.i. as described in experimental procedures. **f** *Pa*-induced cell detachment was investigated by nucleus count after Hoechst labeling. Statistical differences with NI were established with Student's *t* test: * $p = 0.01$; ** $p < 0.003$; *** $p < 0.0001$; # $p = 0.29$. Data are representative of 3–8 independent experiments

Infection with *Pa*-S in which ExoS was mutated in its GAP or ADPRT domain indicated that the GAP domain alone has no effect, whereas the ADPRT domain is responsible for the entire toxic activity (Fig. 1c). Similar experiments were done with activity domain mutants of ExoT. Our data show that the ExoT ADPRT domain has cell retraction effects comparable to *Pa*-T, however its GAP domain induced a lower but significant cell retraction (Fig. 1d). As previously reported, ExoT undergoes auto-ADP-ribosylation and inactivation of its GAP domain [21]. As the cell retraction promoting activity of the two domains is not additive, it is likely that the GAP domain is inactivated in native ExoT.

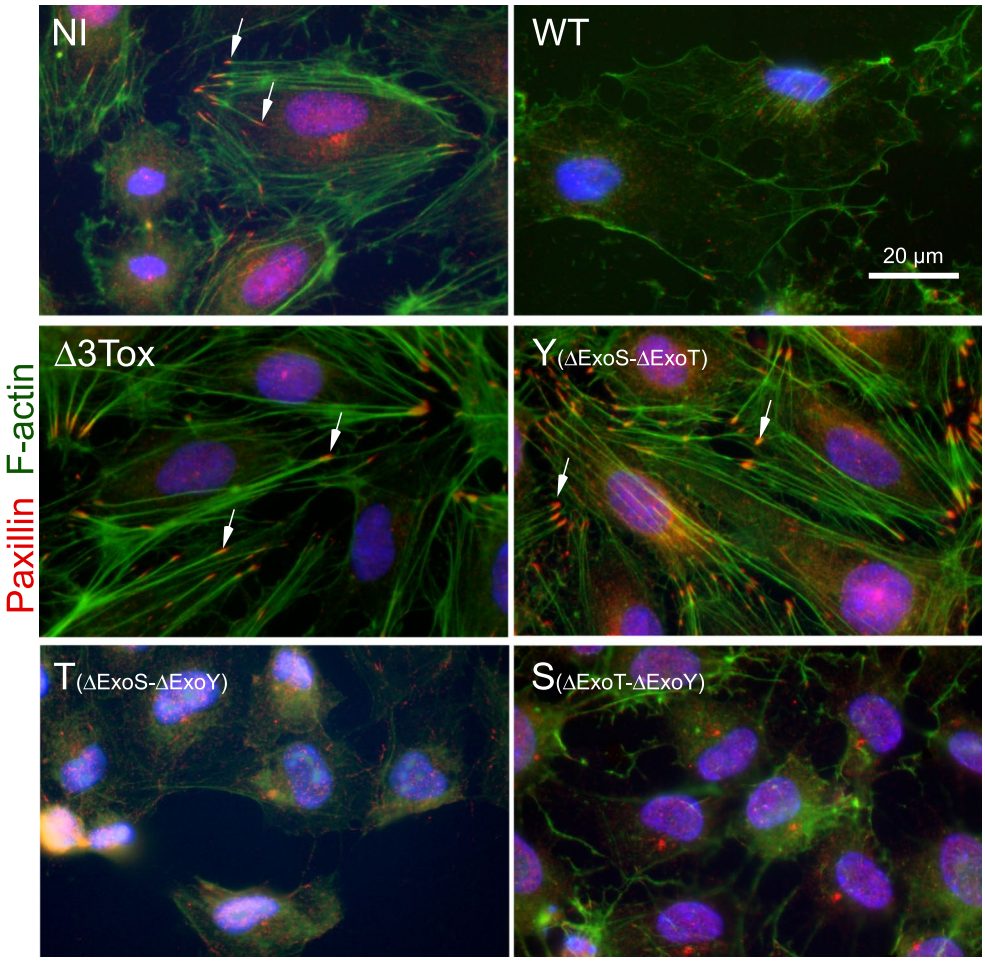

Fig. 2 Disruption of actin cytoskeleton and focal contacts during cell infection. Images of focal adhesions (paxillin in *red*) and actin filaments (F-actin labeled with phalloidin in *green*) of HUVECs either non-infected (NI) or infected with *Pa*-WT (WT), *Pa*-Δ3Tox (Δ3Tox), *Pa*-Y (Y), *Pa*-T (T), or *Pa*-S (S). Nuclei are in *blue*. *Arrows* point to focal adhesions. Images are representative of numerous infected cells

Surprisingly, the double-deletion mutant Δ*ExoS*–Δ*ExoT*, expressing only ExoY (*Pa*-Y), promoted slight but consistent cell spreading (Fig. 1b). To verify that ExoY was indeed injected in infected endothelial cells we measured cAMP levels in host cells, as this toxin is endowed with adenylate cyclase activity (Fig. 1e). Infection with *Pa*-Y significantly increased cAMP levels in HUVECs, suggesting that ExoY was effectively injected, while *Pa*-Δ*3Tox*, *Pa*-S and *Pa*-T had no effects. Interestingly, infection with *Pa*-WT did not increase cAMP levels in endothelial cells, but it secretes ExoY at similar levels as *Pa*-Y [35]. It is likely that simultaneous injection of the two other toxins interplays with ExoY signaling.

We then investigated whether infection with *Pa* had an effect on cell adhesion by counting adherent cells at late post-infection time (4.5 h post-infection). As shown in Fig. 1f, cell retraction was followed by cell detachment indicating that both cell morphology and adhesion were affected by *P. aeruginosa* exotoxins. No necrotic cell death was detected even at late time points ($t = 4$ h) by ethidium bromide permeability assay (not shown).

P. aeruginosa induces actin filament and focal adhesion disruptions

We then examined the actin cytoskeleton and focal adhesion states after *Pa* infection. Both actin filaments (in green) and focal adhesions (visualized by paxillin in red) were disrupted when cells were infected with *Pa*-WT, *Pa*-T, or *Pa*-S, but not by *Pa*-Y or *Pa*-Δ*3Tox* (Fig. 2). To further examine the process of actin filament disruption, HUVECs were transfected with Lifeact-GFP in order to follow the actin filament dynamics during infection by videomicroscopy. In mock-infected cells, actin filaments were stable (movie in Online Resource 6, selected frames in Fig. 3a), whereas they gradually disappeared when infected with *Pa*-WT (movie in Online Resource 7; selected frames in Fig. 3b). Similar data were obtained when cells were infected with *Pa*-S or *Pa*-T (movies in Online Resources 8, 9).

To examine the behavior of focal adhesions during the infection process, cells were transfected with vinculin-GFP and Lifeact-RFP, then infected with *Pa*-WT. Videomicroscopy analysis revealed that F-actin and focal adhesions were disrupted simultaneously (movie in Online Resource

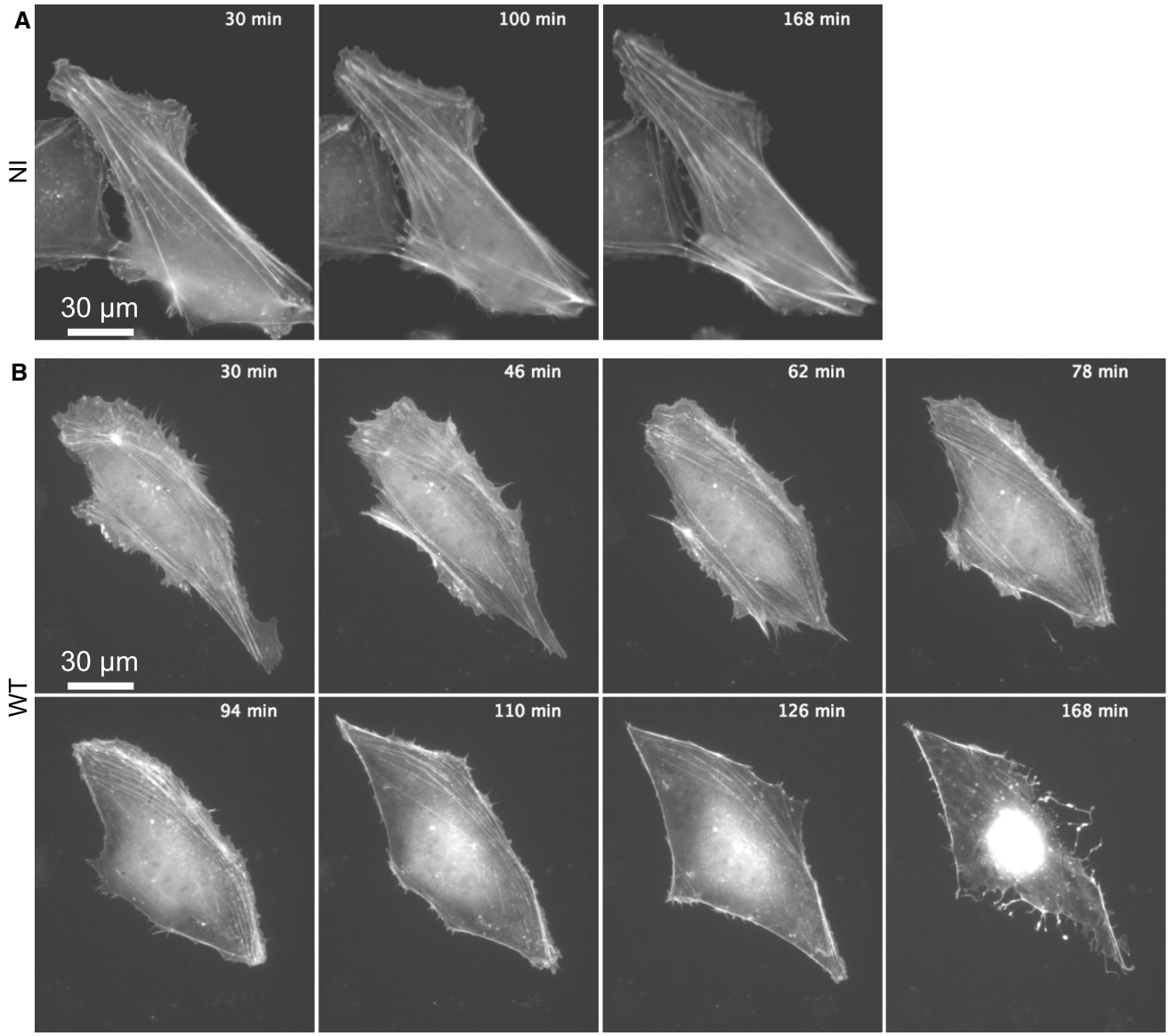

Fig. 3 Kinetics of actin filament disruption during infection. **a** HUVECs were transfected with Lifeact-EGFP and mock-infected with LB 24 h later. **b** HUVECs were transfected with Lifeact-EGFP and infected with *P. aeruginosa* WT 24 h later. Videomicroscopy images of EGFP labeling were taken from Online Resources 6 and 7, respectively. Time post-infection is indicated. Infected cells exhibit progressive loss of actin fibers, while the actin cytoskeleton was stable in mock-infected cells. Images are representative of at least 40 different PAO1-infected cells that were observed under these conditions. Retraction was consistently preceded by cytoskeleton collapse

10), consistent with the known interdependence of both structures [36]. Similar data were obtained with *Pa*-S and *Pa*-T (not shown).

FAK activity is altered during *P. aeruginosa* infection

Integrins within focal adhesions are associated with signaling molecules, such as focal adhesion kinase (FAK), a tyrosine kinase that acts as a transduction platform for outside-in and inside-out signalings [22, 37]. To obtain insight on signaling events leading to endothelial cell-matrix adhesion breakdown, we examined FAK activity by monitoring its tyrosine phosphorylation levels. At the beginning of the adhesion process, FAK autophosphorylated on Y397. Phospho-Y397 is a binding and activation site for Src that in turn phosphorylates FAK on various tyrosine's, including Y576 [37]. As early as 2 h post-infection, we observed a dramatic dephosphorylation of FAK at its autophosphorylation site Y397 and its Src-dependent phosphorylation site Y576 (Fig. 4a). Both processes were equally elicited by wild-type, ExoT-, or ExoS-producing strains (Fig. 4b, c). Thus, FAK is similarly deactivated by cell intoxication with ExoS or ExoT.

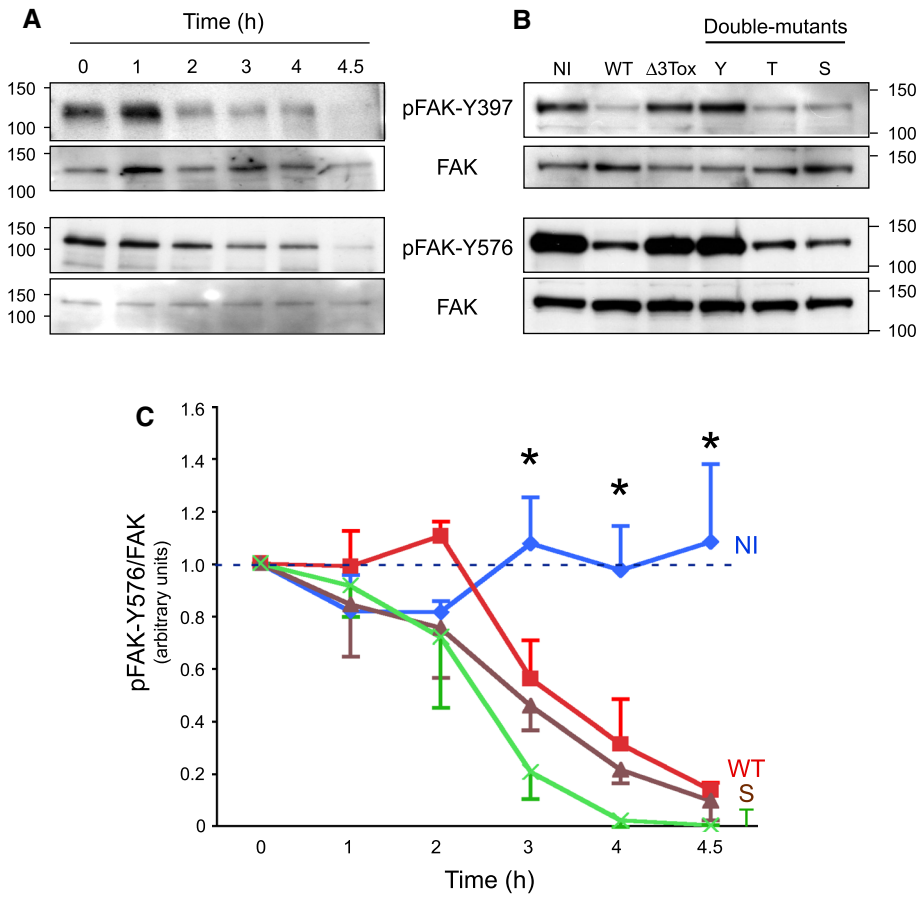

Fig. 4 FAK phosphorylation status in infected cells. **a**, **b** Western-blot analysis of FAK phosphorylation levels on Y397 and Y576. **a** Analysis was performed at different time points of infection with *Pa*-WT or **b** after 4 h of infection with *Pa*-WT (WT), *Pa*-Δ3Tox (Δ3Tox), *Pa*-Y (Y), *Pa*-T (T), or *Pa*-S (S); *NI*, non-infected. Molar weights are indicated. **c** Kinetics experiments were performed as in **a**, and pFAK-Y576 content was measured by Western blot for non-infected cells (NI) or cells infected with *Pa*-WT, *Pa*-S or *Pa*-T. pFAK-Y576 signals were quantified and normalized by FAK signals using ImageJ software. Analysis was performed for three independent experiments for each condition. Data represent the averaged pFAK-Y576/FAK signal ratio (+SEM). *Asterisk* from $t = 3$ h, data between non-infected cells and cells infected with either strain were significantly different ($p < 0.05$; two-sided Student's *t* test)

Altogether, we show that FAK inactivation was triggered by ExoS and ExoT and paralleled focal adhesion disruption.

Alteration of the Lim kinase-cofilin pathway during infection

To explain the dismantlement of the actin cytoskeleton in such a short period of time (90–180 min), we evaluated the phosphorylation status of cofilin, an actin severing and depolymerization factor that is inactivated by phosphorylation. We indeed observed a time-course dephosphorylation of cofilin when cells were infected with either *Pa*-WT, *Pa*-S, or *Pa*-T (Fig. 5a–c). These features are consistent with the generally accepted role of cofilin in actin fiber fragmentation [38].

Cofilin activity is downregulated by Lim kinase, which is itself activated by phosphorylation [38]. The phosphorylation levels of Lim kinase progressively decreased when HUVECs were infected with *Pa*-WT (Fig. 5d), and this decrease was equally produced by *Pa*-WT, *Pa*-T, or *Pa*-S (Fig. 5e), reinforcing the hypothesis of a Lim kinase-cofilin-actin pathway alteration during infection. Lim kinase has a potent role in maintaining the actin cytoskeleton integrity in endothelial cells, as illustrated by incubation of HUVECs with the recently identified Lim kinase inhibitor Pyr1 [39]. This induced a similar disruption of stress fibers (Fig. 5f), but no cell retraction probably because Pyr1 does not recapitulate all *P. aeruginosa* toxic effects.

Cofilin-dependent actin filament disruption requires inactivation of both Rho and Rac-Cdc42 pathways

Lim kinase may be activated either by the Rac, Cdc42-PAK1, PAK4 axis, or by the RhoA-Rho kinase axis [40]. These Rho G-proteins are known targets of ExoS and ExoT, either through their GAP and/or ADPRT activities [3]. We thus measured Rho protein activities during infection to determine which initial mechanism could lead to perturbation of the Lim kinase-cofilin pathway. RhoA activity was dramatically increased at 1 h post-infection and then decreased to minimal levels at later time points (Fig. 6a). Similar results were obtained with the phosphorylation levels of MYPT (Fig. 6b), a specific downstream effector of the RhoA-Rock pathway [40], thus confirms that RhoA activity is biphasic during infection. ExoT or ExoS individually induced a decrease in RhoA activity at 3-h post-infection (Fig. 6a).

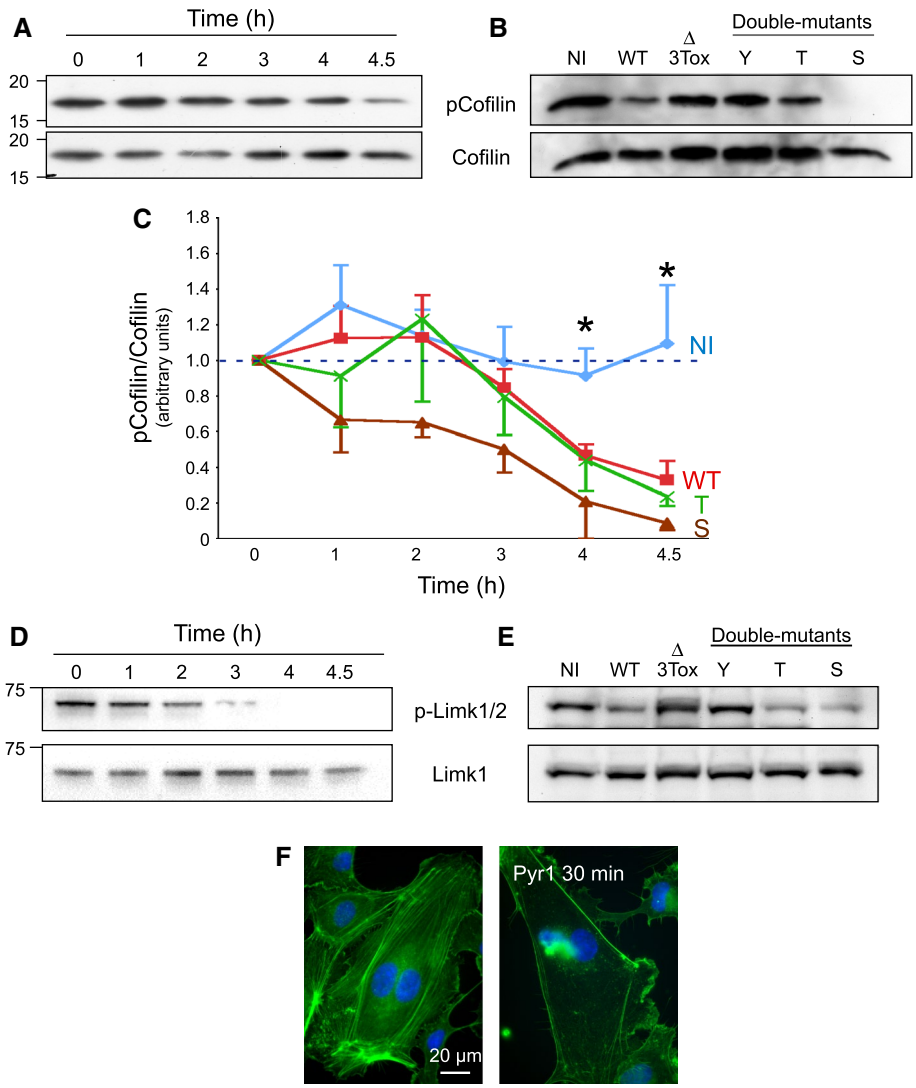

Fig. 5 ExoS and ExoT affect cofilin and Lim kinase phosphorylation levels. **a** Western-blot analysis of phospho-cofilin during *Pa*-WT infection of HUVECs. **b** Phospho-cofilin levels after 4.5 h of infection with *Pa*-WT (WT), *Pa*-Δ3Tox (Δ3Tox), *Pa*-Y (Y), *Pa*-T (T), or *Pa*-S (S); *NI*, non-infected. **c** Kinetics experiments were performed as in **a**, and phospho-cofilin content was measured by Western blot for non-infected cells (NI) or cells infected with *Pa*-WT, *Pa*-S, or *Pa*-T. Phospho-cofilin signals were quantified and normalized with cofilin signals using ImageJ software. Analysis was performed for three independent experiments for each condition. Data represent the averaged phospho-cofilin/cofilin signal ratio (+SEM). *Asterisk* from $t = 4$ h, data between non-infected cells and cells infected with *Pa*-WT or *Pa*-S were significantly different ($p < 0.05$; two-sided Student's t test). Significance was reached at $t = 4.5$ h for infection with *Pa*-T. **d** Kinetics study of phospho-Lim kinase levels after infection with *Pa*-WT. **e** Phospho-Lim kinase levels, indications as in **b**. **f** HUVECs were incubated for 30 min with 62.5 nM Pyr1 and labeled with phalloidin

Rac-active and Cdc42-active levels decreased, starting at 1- and 3-h post-infection, respectively (Fig. 6c, d). At 3-h post-infection, Rac1 and Cdc42 were similarly inhibited by *Pa*-T and *Pa*-S. Altogether, these features indicate that ExoS and ExoT can similarly inactivate the Rho proteins, whereas ExoY has no effect or cannot even activate Cdc42.

As Rac is known to activate cell ruffling and lamellipodia formation [40], we wondered whether *Pa*-induced Rac inactivation correlated with ruffling interruption. Therefore, HUVECs were transfected with Lifeact-GFP and infected when cells were sparse as opposed to previous experiments. In these conditions, we observed an interruption in membrane ruffling before the actin cytoskeleton collapsed, as illustrated in the movie from Online Resource 11 and selected frames in Fig. 7a. This was not observed in uninfected cells (Fig. 7a). Cdc42 activation promotes filopodia formation [40]. Using the same experimental conditions but focusing on filopodial extensions, we noticed that intrafilopodial actin collapsed in parallel with intracellular actin filaments (movie in Online Resource 12; selected frames in Fig. 7b).

Moesin inactivation is not required for cell retraction

Ezrin, moesin, and radixin are related proteins, forming the ERM family, that bind actin and have important roles in actin cytoskeleton remodeling [41]. These proteins are ADP-ribosylated by ExoS in epithelial cells, which prevents their activation by phosphorylation. ERM were proposed to be major players in *Pa*-induced cell retraction [20]. In support of this, a dominant active mutant of moesin prevented ExoS-induced cell rounding [20]. As moesin is the main ERM family member expressed in endothelial cells, we examined the phosphorylation status of this protein during infection. As shown in Fig. 8, we did not detect any variation in HUVEC phospho-moesin content, even after long infection time (up to 4.5 h p.i). We conclude that *Pa*-induced actin cytoskeleton collapse is not caused by

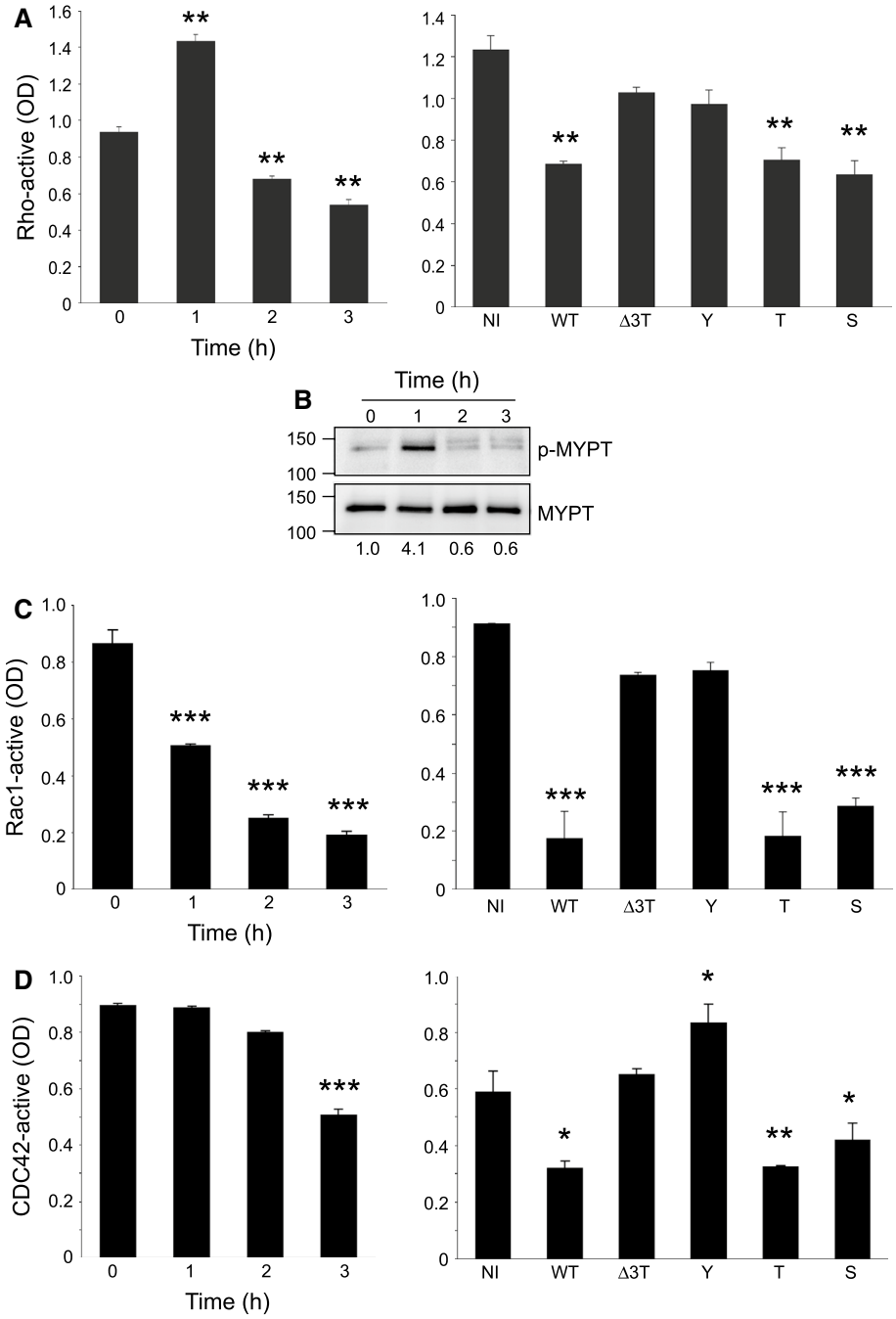

Fig. 6 Rho, Rac, and Cdc42 activities in infected HUVECs. **a**, **c**, **d** The GTP-linked forms of Rho (**a**), Rac1 (**c**), and Cdc42 (**d**) were measured by specific G-LISA kits either in kinetics with *Pa*-WT (left panels) or after infection (3-h p.i.) with *Pa*-WT (WT), *Pa*-Δ3Tox (Δ3Tox), *Pa*-Y (Y), *Pa*-T (T), or *Pa*-S (S); *NI*, non-infected (*right panels*). Data are representative of 2–3 independent experiments performed in triplicates. G-LISA data were confirmed by pull-down experiments (not shown). Statistical differences with T0 or NI were established by Student's *t* test: * $p = 0.02$; ** $p < 0.001$; *** $p < 0.0001$. **b** Kinetics of phospho-MYPT levels after infection with *Pa*-WT. Molar weights are indicated on the left. Phospho-MYPT/MYPT ratios are indicated below each lane

moesin inactivation in endothelial cells as opposed to epithelial cells.

The active forms of Rac, RhoA, Lim kinase, and mDia2 decreased Pa-induced cell retraction

We next evaluated the effects of the constitutively active forms of Rho and Rac on *Pa*-induced cell retraction. HUVECs were transfected with plasmids encoding EGFP, EGFP-RhoV14, or EGFP-RacV12, and 24 h later infected with *Pa*-WT. Transfection with RhoV14 or RacV12 had a striking effect on *Pa*-induced cell retraction (Fig. 9a) thus confirming that the activity of either RhoA or Rac1 is sufficient to impede cell retraction.

We then wondered whether the transient Rho activation reported in Fig. 6a, b was caused by the rapid Rac inactivation observed in Fig. 6c, because these two GTPases are known to negatively regulate each other [42]. Therefore, Rho activity in EGFP-RacV12-transfected cells was measured at different time points post-infection (Fig. 9b) and the results show that the transient Rho upregulation detected in EGFP-transfected cells was abolished when RacV12

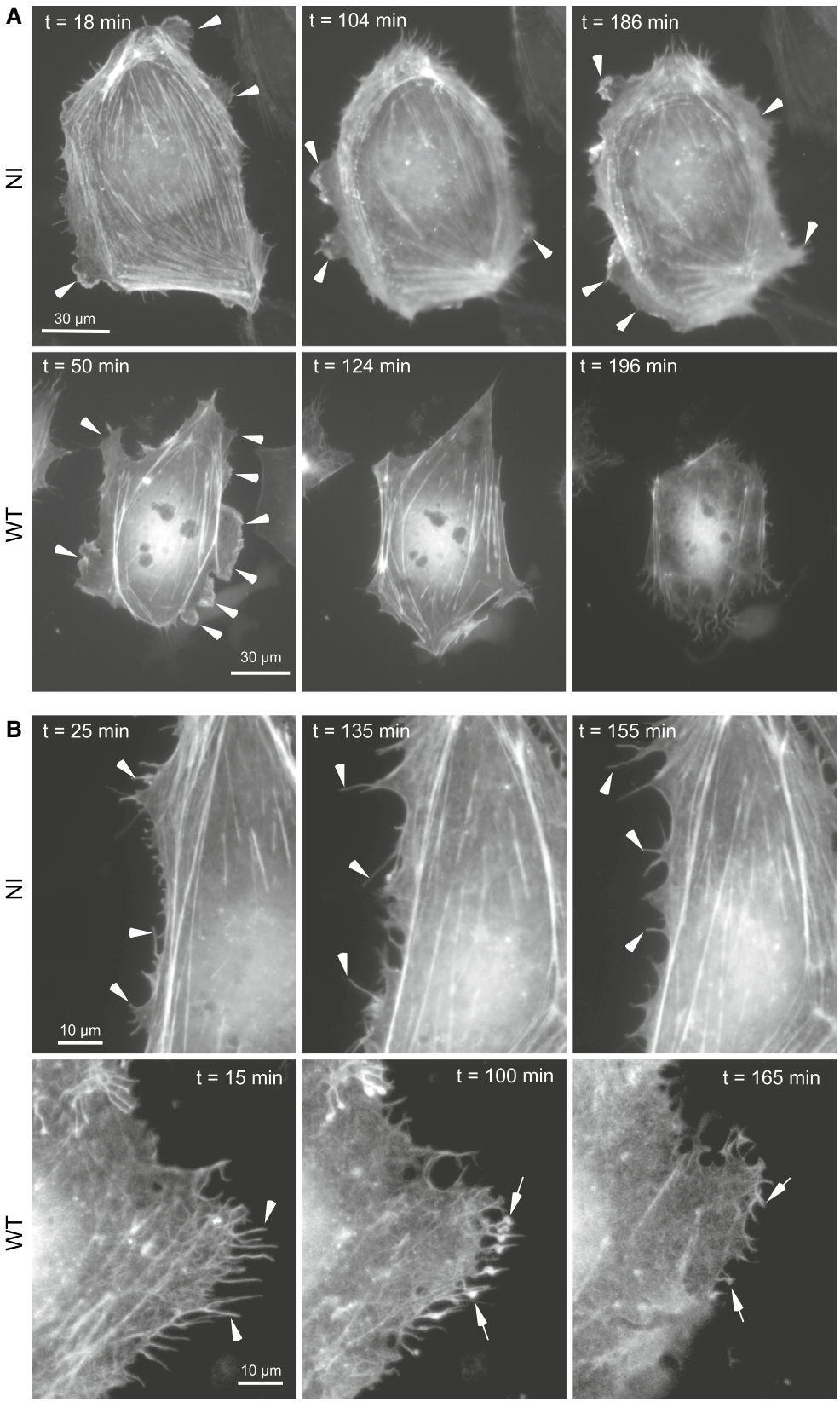

Fig. 7 Lamellipodial and filopodial activities are inhibited in infected HUVECs. Sparse cells were transfected with Lifeact-EGFP and either infected 24 h later with *Pa*-WT (WT) or were non-infected (NI). Videomicroscopy images of infected cells were taken from movies in Online Resources 11, 12. **a** At the early phase of infection ($t = 50$ min) membrane ruffling is highly visible (*arrowheads*) in infected and uninfected conditions. In infected cells at $t = 124$ min, ruffling activity is abolished but stress fibers are still present in infected cells; at $t = 196$ min, stress fibers are disrupted and the cell is retracting. **b** The images focus on cells forming numerous filopodia. During infection, filopodia regress (*arrows*) via collapse of the intrafilopodial actin filaments

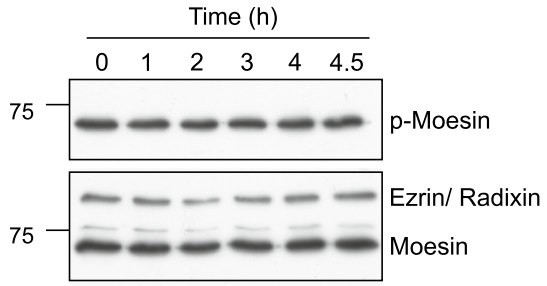

Fig. 8 *P. aeruginosa* infection has no effect on phospho-moesin levels. Western-blot analysis of phospho-moesin during *Pa*-WT infection of HUVECs. Total moesin, as well as ezrin and radixin, are shown in control

was overexpressed. These features suggest that Rac down-regulation is required or promotes transient Rho activity increase.

In another set of experiments, we transfected the constitutively active forms of either Lim kinase (myc-LimK-T508EE) or mDia2 (EGFP-mDia2-FH1FH2). mDia2 is a member of the form in family whose major function is to promote actin polymerization and that is a common target of Rho GTPases [43]. Both Lim kinase and mDia2 transfections significantly limited *Pa*-induced cell retraction compared to EGFP control (Fig. 9c), but their effects were not as important as observed for Rho- or Rac-active transfections. Altogether, our data are consistent with the notion that cell retraction impediment requires both inhibition of actin filament severing and activation of actin polymerization.

To further establish that Lim kinase is dephosphorylated during infection because of Rho GTPase inactivation, we determined Lim kinase phosphorylation status in HUVECs overexpressing EGFP or RacV12 (Fig. 9d).

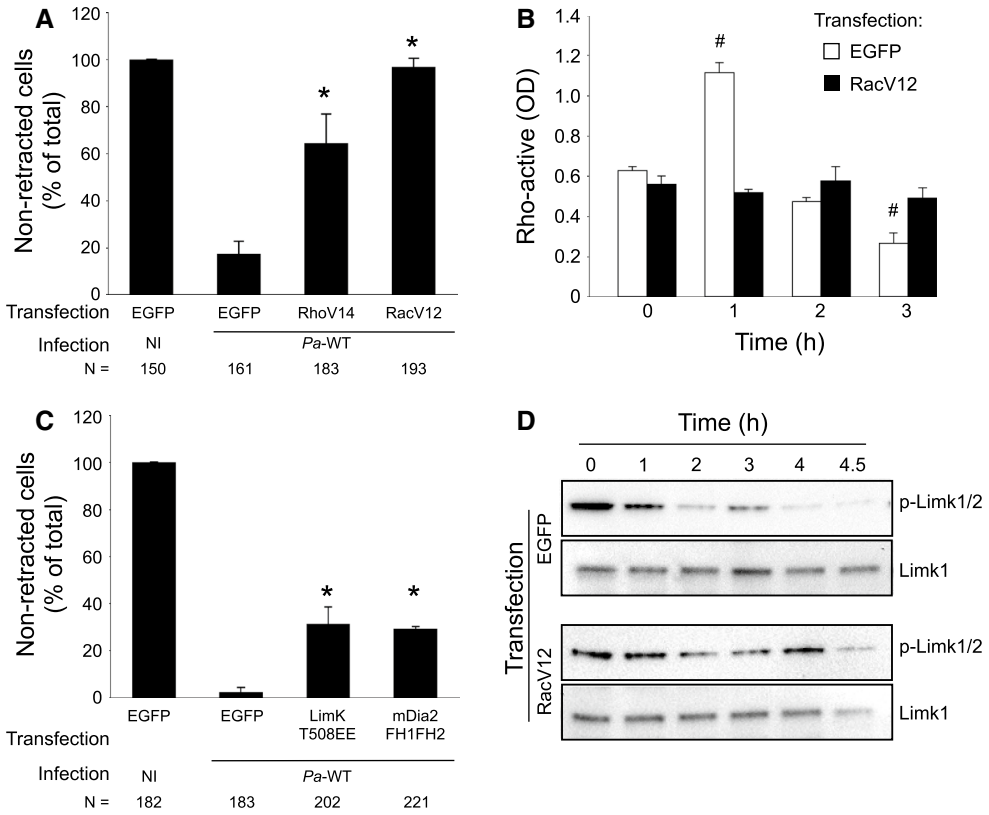

Fig. 9 Effects of the active forms of Rho, Rac, Lim kinase, and mDia2 on Pa-induced cell retraction. **a** The constitutively active forms of Rho (EGFP-RhoV14), Rac (EGFP-RacV12) were transfected in HUVECs. Plasmid pEGFP was used in control. After 24 h, cells were either infected with *Pa*-WT or remained non-infected (NI), as indicated. Cells were then fixed, labeled with phalloidin, as well as myc for LimK transfection. Transfected cells were selected by EGFP or myc expression using ImageJ software, and were then classified in retracted or non-retracted cells in three different areas at low magnification. Data are presented as the mean + SD of cell percentage of each category in total image area. The total number of counted cells is indicated below each condition. **b** HUVECs were transfected with either pEGFP or RacV12 and Rho activity was measured at different time points post-infection with a Rho-G-LISA kit. **c** Experiment analogous to **a** with overexpression of LimK (LimK-T508EE-myc) and mDia2 (EGFP-mDia2-FH1FH2). Data are representative of 2–4 independent experiments. **d** HUVECs were transfected with either pEGFP or EGFP-RacV12 and infected with *Pa*-WT, as above. Phospho-Lim kinase and Lim kinase levels were analyzed by Western blot at different time points. **a**, **c** Statistical differences with EGFP-transfected and infected cells were established with χ^2 test: * $p < 0.0001$. **b** Statistical differences with data at time $t = 0$ were determined by Student's t test: $^{\#}$ $p < 0.001$

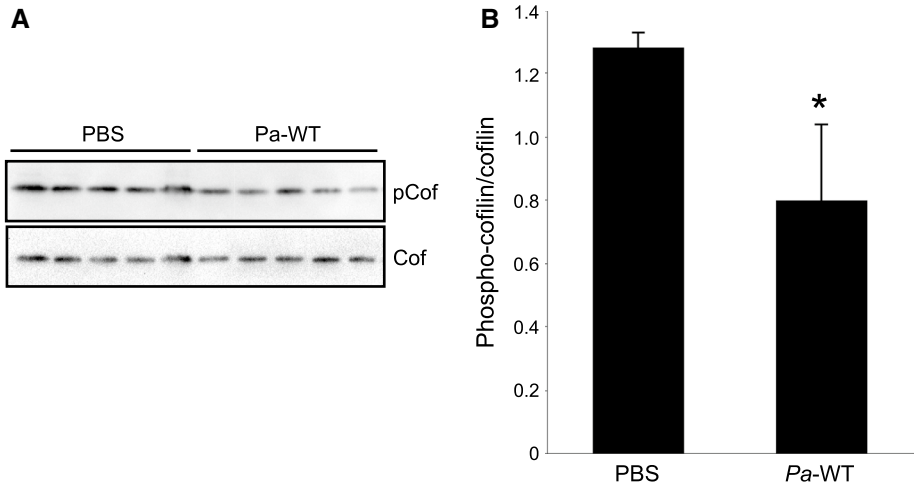

Fig. 10 Decreased phospho-cofilin levels in Pa-infected mice. Acute pneumonia was induced by *Pa* inhalation, as described in experimental procedures. Sixteen hours later, mice were euthanized; lung protein extracts were prepared and analyzed by Western blotting using phospho-cofilin (pCof) and cofilin (Cof) antibodies. **a** Data show analysis of five mouse lungs infected by *Pa*-WT (PAO1F) or mock-infected with PBS. **b** Histograms represent the average (+SEM) of phospho-cofilin/cofilin ratio for $n = 5$ mice per condition. Statistical difference was established by two-sided Student's t test: $p = 0.007$. Data shown here are representative of two independent experiments

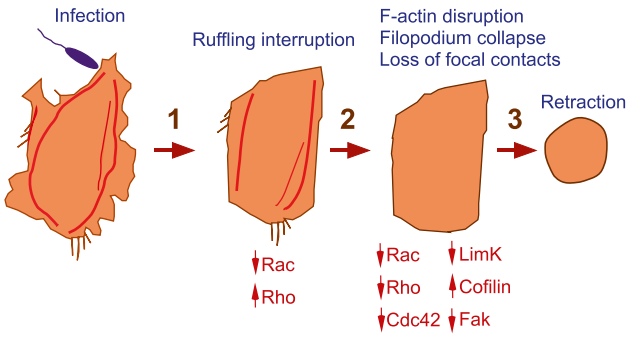

Fig. 11 *P. aeruginosa*-induced cell retraction is a three-step process. In the initial phase of intoxication, Rac activity decreases while Rho activity increases, leading to ruffling interruption. In the second step, all Rho GTPases are inhibited, triggering cofilin activation and actin filament cleavage. In parallel, focal adhesions are disrupted and FAK is de-activated. As a result, the cell retracts at the end of the process

In EGFP-expressing cells, phospho-Lim kinase levels decreased progressively, like in Fig. 5d. In contrast, phospho-Lim kinase signals were detected until 4.5 h p.i. in RacV12-expressing cells. Thus, ectopic expression of at least one Rho GTPase is sufficient to maintain Lim kinase active during infection.

Decreased cofilin phosphorylation in Pa-infected lungs

To examine whether cofilin activation is indeed a mechanism occurring during in vivo infection, we analyzed cofilin phosphorylation levels in lungs of mice with acute pneumonia. A suspension of *Pa*-WT (5.10^6/mice) was instilled in the mouse lungs by inhalation and mice were euthanized 16 h later. Proteins from lung extracts were analyzed by Western blot with phospho-cofilin and cofilin antibodies (Fig. 10). Our results exhibited a significant decrease in cofilin phosphorylation in total lung extracts, thus demonstrating that cofilin is activated in infected lung cells.

Discussion

This work was motivated by several considerations: (1) Although the Rho GTPases, the ERM and Crk proteins are known targets of *P. aeruginosa* T3S effectors, the importance of their respective inactivation in cell rounding/retraction remained elusive. (2) Most of the previous in vitro studies were made with carcinoma or leukemic cell lines with altered signaling pathways instead of primary cells. (3) A limited number of studies addressed the mechanisms of *P. aeruginosa* intoxication of endothelial cells. (4) As far as we know, there have been no precise kinetic studies deciphering the various steps of cytoskeletal modifications during the intoxication process. Here, we show that various primary endothelial cell types are highly sensitive to *P. aeruginosa* T3SS and respond by a dramatic retraction, while this phenomenon in epithelial cells is more related to cell rounding (Online Resource 4). The mutant injecting only ExoS was consistently more potent than the wild-type strain expressing all three toxins, suggesting a possible interplay between toxins. ExoT elicited a slightly milder retraction than the wild-type and ExoY did not induce retraction and even increased cell spreading (Fig. 1).

The absence of ExoY retraction activity is in agreement with Ganter et al. [32] but contradicts the data obtained by Sayner et al. [33]. ExoY may thus have differential effects depending on host species (rat versus human) or strain background (PA103 versus PAO1F).

Actin-mediated cellular processes, such as formation of filopodia, lamellipodia and stress fibers, require the coordinated and local actions of polymerizing factors, including the mDia formins and the Arp2/3 complex, as well as depolymerizing and severing agents such as cofilin [40, 44]. There is a considerable interplay between the numerous factors regulating F-actin and focal adhesion dynamics [36, 45–47]. Although a substantial effort has been made to decipher the different regulation pathways and events controlling cell migration, the steps leading to pathological cell retraction are poorly understood.

The ADPRT activities of ExoS and ExoT are major promoters of cell retraction and both seem to produce the same effect (Fig. 1c, d) although ExoS and ExoT ADPRT activities are known to target different protein substrates [48]. ExoT GAP domain alone was also sufficient to trigger cell retraction, while ExoS GAP domain was ineffective (Fig. 1c, d). However, ExoT auto-ADP-ribosylates and inactivates its GAP domain [21], suggesting that ExoT GAP domain is also ineffective in the wild-type strain.

ExoS and ExoT individually inhibited the Rho GTPases, as well as Lim kinase and FAK (Figs. 4, 5, 6). The fact that Lim kinase inhibition during infection originates from Rho GTPase inactivation was further demonstrated by the persistence of a phospho-Lim kinase signal in RacV12-overexpressing cells (Fig. 9d). It has been amply demonstrated that actin fibers and focal adhesions are interdependent structures [36]. Focal adhesions need actin tension to be maintained as several of their components, including integrins, talin and p130Cas are sensitive to strengths exerted on the complex by actin filaments [45–47]. When actin tension decreases, either by actin filament severing or myosin light chain inhibition, the focal adhesion complex is disrupted and FAK phosphorylation at Y397 is greatly diminished. Conversely, the FAK-p130Cas-Crk pathway is a major route of Rac activation [22]. Therefore, Rac inhibition may occur either directly by the ADPRT domain of ExoS or through Crk inactivation by the ADPRT domain of ExoT or by the GAP domain of ExoT, as previously described in epithelial cells [23, 49]. Cdc42 may also be inactivated by ExoS ADPRT activity or remaining ExoT GAP activity [14, 49]. In *P. aeruginosa*-infected HUVECs, Cdc42 appeared to be inhibited at a lower rate and later than Rac (Fig. 6). Finally, Rho inactivation may be indirectly induced by negative feedback from focal contact disruption.

Importantly, we observed a sequential inactivation of all three GTPases. Rac was rapidly and dramatically deactivated as shown by Rac activity assay in correlation with the inhibition of cell ruffling noted in videomicroscopy (Fig. 7a). In contrast, Rho activity first increased and then returned to minimal level, as monitored by Rho activity assay and MYPT phosphorylation level (Fig. 6). Cdc42 activity decreased together with that of Rho (Fig. 6), a process that can be visualized by the retraction of filopodia simultaneously with the disruption of intracellular actin fibers (Fig. 7b). The initial burst of Rho activity is likely to be caused by Rac inactivation, as artificial maintenance of Rac activity in infected cells prevented this phenomenon (Fig. 9b).

Altogether, our data clearly show that cell retraction occurred after disruption of the actin cytoskeleton and focal adhesions. Ganter et al. [32] reported the inactivation of Rac and the induction of Rho activity together with an increase in stress fibers 10 min after *P. aeruginosa* infection of endothelial cells. Similarly, Kazmierzack et al. [50] showed that RhoA was activated in *P. aeruginosa*-infected epithelial cells. Our data at 1 h post-infection are in agreement with theirs. However, we extended this analysis and noted that Rho activation is only transient and rapidly followed by inactivation. Thus in later time points, all three GTPases were inactivated and this event was accompanied by progressive actin cytoskeleton disruption. Our results on cell retraction and monolayer permeability are also consistent with the increases in monolayer permeability that Ganter et al. [32] observed at 3 h p. i.

Microtubules were also destabilized in infected HUVECs (Online Resource 13), a process known to favor cell retraction [51, 52]. We therefore propose an intoxication model in three steps (Fig. 11), in which loss of monolayer integrity is caused by cytoskeleton depletion instead of stress fiber-mediated cell contraction. Similarly, inactivation of all three GTPases by *Staphylococcus aureus* toxins is required for cell retraction [53].

Interestingly, ectopic expression of the active forms of Rho or Rac strikingly limited cell retraction (Fig. 8). Rac overexpression was already shown to impede ExoT-induced cell rounding in epithelial cells [23]. Both Rho and Rac have many downstream targets including the Lim kinase-cofilin axis and formins that function as potent stimulators of actin nucleation and elongation [38, 54]. mDia1 formin is a specific Rho effector while mDia2 and mDia3 are activated by all Rho GTPases [43]. We thus transfected HUVECs with plasmids encoding the active forms of Lim kinase or mDia2, as mDia2 is one of the most promiscuous effectors of Rho GTPases to see whether they could impede *P. aeruginosa*-induced cell retraction. Over expression of either protein incompletely but significantly impacted cell retraction (Fig. 9). This suggests that total prevention of cell retraction requires both the anti-severing and actin polymerization activities of Rho GTPases.

Members of the ezrin-radixin-moesin (ERM) protein family, acting as molecular cross linkers between actin filaments and proteins anchored in the cell membrane, were shown to be primary targets of ExoS ADPRT activity [15]. ADP-ribosylation of these proteins prevents their phosphorylation thereby precluding their transition to an active conformation [20]. As previously mentioned, inhibition of ERM proteins is thought to be a major event in *P. aeruginosa*-induced epithelial cell rounding [20]. Moesin is the most abundantly expressed protein of the family in endothelial cells; we thus examined moesin phosphorylation levels and observed that it was not altered by infection, suggesting that ExoS and ExoT do not operate through this pathway in this cell type to induce retraction (Fig. 8). Another possible explanation is that Maresso et al. [20] infected subconfluent HeLa cells (70 % confluent) but in our study infection occurred in confluent HUVECs designed to reconstitute the endothelium monolayer. It is also possible that the pool of moesin was already highly phosphorylated at that stage and insensitive to ADP-ribosylation.

In conclusion, we demonstrated that inactivation of all three Rho GTPases is required for T3S-induced endothelial cell retraction, but ERM proteins are probably not affected by the three exotoxins. The inactivation kinetics are different between Rho, Rac and Cdc42. Notably, cytoskeleton and focal adhesion disruption takes place through the Lim kinase-cofilin pathway as a consequence of GTPase inactivation. Using a mouse pneumonia model, we showed that cofilin is indeed activated in the infected lungs. Although ExoS and ExoT have different protein substrates, they produce comparable effects in endothelial cells by disarming similar signaling pathways.

Acknowledgments This work was supported by grants from the Commissariat à l'Energie Atomique, the Institut National de la Santé et de la Recherche Médicale, the Centre National de la Recherche Scientifique and Joseph Fourier University. Part of this work was also supported by the Alliance pour les sciences de la VIE et de la SANté program in infectiology. We thank Anne-Sophie Ribba for the moesin antibody, Laurence Lafanechère for Pyr1, Cécile Gauthier-Rouvière, Kenzaku Mizuno, Roland Wedlich-Soldner, Hélène Delanoë-Ayari and Gregg Gunderson for expression plasmids, and Arne Rietsch for *Pseudomonas aeruginosa* mutant strains.

References

1. Deng Q, Barbieri JT (2008) Molecular mechanisms of the cytotoxicity of ADP-ribosylating toxins. Annu Rev Microbiol 62:271–288
2. Engel J, Balachandran P (2009) Role of *Pseudomonas aeruginosa* type III effectors in disease. Curr Opin Microbiol 12(1):61–66
3. Hauser AR (2009) The type III secretion system of *Pseudomonas aeruginosa*: infection by injection. Nat Rev 7(9):654–665
4. Vance RE, Rietsch A, Mekalanos JJ (2005) Role of the type III secreted exoenzymes S, T, and Y in systemic spread of *Pseudomonas aeruginosa* PAO1 in vivo. Infect Immun 73(3):1706–1713
5. Goehring UM, Schmidt G, Pederson KJ, Aktories K, Barbieri JT (1999) The N-terminal domain of *Pseudomonas aeruginosa* exoenzyme S is a GTPase-activating protein for Rho GTPases. J Biol Chem 274(51):36369–36372
6. Pederson KJ, Vallis AJ, Aktories K, Frank DW, Barbieri JT (1999) The amino-terminal domain of *Pseudomonas aeruginosa* ExoS disrupts actin filaments via small-molecular-weight GTP-binding proteins. Mol Microbiol 32(2):393–401
7. Kazmierczak BI, Engel JN (2002) *Pseudomonas aeruginosa* ExoT acts in vivo as a GTPase-activating protein for RhoA, Rac1, and Cdc42. Infect Immun 70(4):2198–2205
8. Krall R, Schmidt G, Aktories K, Barbieri JT (2000) *Pseudomonas aeruginosa* ExoT is a Rho GTPase-activating protein. Infect Immun 68(10):6066–6068
9. Barbieri AM, Sha Q, Bette-Bobillo P, Stahl PD, Vidal M (2001) ADP-ribosylation of Rab5 by ExoS of *Pseudomonas aeruginosa* affects endocytosis. Infect Immun 69(9):5329–5334
10. Coburn J, Dillon ST, Iglewski BH, Gill DM (1989) Exoenzyme S of *Pseudomonas aeruginosa* ADP-ribosylates the intermediate filament protein vimentin. Infect Immun 57(3):996–998
11. Coburn J, Gill DM (1991) ADP-ribosylation of p21ras and related proteins by *Pseudomonas aeruginosa* exoenzyme S. Infect Immun 59(11):4259–4262
12. Fraylick JE, Riese MJ, Vincent TS, Barbieri JT, Olson JC (2002) ADP-ribosylation and functional effects of *Pseudomonas* exoenzyme S on cellular RalA. Biochemistry 41(30):9680–9687
13. Ganesan AK, Vincent TS, Olson JC, Barbieri JT (1999) *Pseudomonas aeruginosa* exoenzyme S disrupts Ras-mediated signal transduction by inhibiting guanine nucleotide exchange factor-catalyzed nucleotide exchange. J Biol Chem 274(31):21823–21829
14. Henriksson ML, Sundin C, Jansson AL, Forsberg A, Palmer RH, Hallberg B (2002) Exoenzyme S shows selective ADP-ribosylation and GTPase-activating protein (GAP) activities towards small GTPases in vivo. Biochem J 367(Pt 3):617–628
15. Maresso AW, Baldwin MR, Barbieri JT (2004) Ezrin/radixin/moesin proteins are high affinity targets for ADP-ribosylation by *Pseudomonas aeruginosa* ExoS. J Biol Chem 279(37):38402–38408
16. McGuffie EM, Frank DW, Vincent TS, Olson JC (1998) Modification of Ras in eukaryotic cells by *Pseudomonas aeruginosa* exoenzyme S. Infect Immun 66(6):2607–2613
17. Riese MJ, Wittinghofer A, Barbieri JT (2001) ADP ribosylation of Arg41 of Rap by ExoS inhibits the ability of Rap to interact with its guanine nucleotide exchange factor, C3G. Biochemistry 40(11):3289–3294
18. Rocha CL, Rucks EA, Vincent DM, Olson JC (2005) Examination of the coordinate effects of *Pseudomonas aeruginosa* ExoS on Rac1. Infect Immun 73(9):5458–5467
19. Jansson AL, Yasmin L, Warne P, Downward J, Palmer RH, Hallberg B (2006) Exoenzyme S of *Pseudomonas aeruginosa* is not able to induce apoptosis when cells express activated proteins, such as Ras or protein kinase B/Akt. Cell Microbiol 8(5):815–822
20. Maresso AW, Deng Q, Pereckas MS, Wakim BT, Barbieri JT (2007) *Pseudomonas aeruginosa* ExoS ADP-ribosyltransferase inhibits ERM phosphorylation. Cell Microbiol 9(1):97–105
21. Sun J, Barbieri JT (2003) *Pseudomonas aeruginosa* ExoT ADP-ribosylates CT10 regulator of kinase (Crk) proteins. J Biol Chem 278(35):32794–32800
22. Birge RB, Kalodimos C, Inagaki F, Tanaka S (2009) Crk and CrkL adaptor proteins: networks for physiological and pathological signaling. Cell Commun Signal 7:13
23. Deng Q, Sun J, Barbieri JT (2005) Uncoupling Crk signal transduction by *Pseudomonas* exoenzyme T. J Biol Chem 280(43):35953–35960

24. Phillips RM, Six DA, Dennis EA, Ghosh P (2003) In vivo phospholipase activity of the *Pseudomonas aeruginosa* cytotoxin ExoU and protection of mammalian cells with phospholipase A2 inhibitors. J Biol Chem 278(42):41326–41332
25. Sato H, Frank DW, Hillard CJ, Feix JB, Pankhaniya RR, Moriyama K, Finck-Barbancon V, Buchaklian A, Lei M, Long RM, Wiener-Kronish J, Sawa T (2003) The mechanism of action of the *Pseudomonas aeruginosa*-encoded type III cytotoxin ExoU. EMBO J 22(12):2959–2969
26. Hritonenko V, Mun JJ, Tam C, Simon NC, Barbieri JT, Evans DJ, Fleiszig SM (2011) Adenylate cyclase activity of *Pseudomonas aeruginosa* ExoY can mediate bleb-niche formation in epithelial cells and contributes to virulence. Microb Pathog 51(5):305–312
27. Lee VT, Smith RS, Tummler B, Lory S (2005) Activities of *Pseudomonas aeruginosa* effectors secreted by the type III secretion system in vitro and during infection. Infect Immun 73(3):1695–1705
28. Yahr TL, Vallis AJ, Hancock MK, Barbieri JT, Frank DW (1998) ExoY, an adenylate cyclase secreted by the *Pseudomonas aeruginosa* type III system. Proc Natl Acad Sci USA 95(23):13899–13904
29. Le Berre R, Faure K, Fauvel H, Viget NB, Ader F, Prangere T, Thomas AM, Leroy X, Pittet JF, Marchetti P, Guery BP (2004) Apoptosis inhibition in *P. aeruginosa*-induced lung injury influences lung fluid balance. Intensive Care Med 30(6):1204–1211
30. Lange M, Hamahata A, Enkhbaatar P, Esechie A, Connelly R, Nakano Y, Jonkam C, Cox RA, Traber LD, Herndon DN, Traber DL (2008) Assessment of vascular permeability in an ovine model of acute lung injury and pneumonia-induced *Pseudomonas aeruginosa* sepsis. Crit Care Med 36(4):1284–1289
31. Woods DE, Hwang WS, Shahrabadi MS, Que JU (1988) Alteration of pulmonary structure by *Pseudomonas aeruginosa* exoenzyme S. J Med Microbiol 26(2):133–141
32. Ganter MT, Roux J, Su G, Lynch SV, Deutschman CS, Weiss YG, Christiaans SC, Myazawa B, Kipnis E, Wiener-Kronish JP, Howard M, Pittet JF (2009) Role of small GTPases and alphavbeta5 integrin in *Pseudomonas aeruginosa*-induced increase in lung endothelial permeability. Am J Respir Cell Mol Biol 40(1):108–118
33. Sayner SL, Frank DW, King J, Chen H, VandeWaa J, Stevens T (2004) Paradoxical cAMP-induced lung endothelial hyperpermeability revealed by *Pseudomonas aeruginosa* ExoY. Circ Res 95(2):196–203
34. Baldwin MR, Barbieri JT (2005) The type III cytotoxins of yersinia and *Pseudomonas aeruginosa* that modulate the actin cytoskeleton. Curr Top Microbiol Immunol 291:147–166
35. Cisz M, Lee PC, Rietsch A (2008) ExoS controls the cell contact-mediated switch to effector secretion in *Pseudomonas aeruginosa*. J Bacteriol 190(8):2726–2738
36. Tomar A, Schlaepfer DD (2009) Focal adhesion kinase: switching between GAPs and GEFs in the regulation of cell motility. Curr Opin Cell Biol 21(5):676–683
37. Mitra SK, Schlaepfer DD (2006) Integrin-regulated FAK-Src signaling in normal and cancer cells. Curr Opin Cell Biol 18(5):516–523
38. Zigmond SH (2004) Beginning and ending an actin filament: control at the barbed end. Curr Top Dev Biol 63:145–188
39. Prudent R, Vassal-Stermann E, Nguyen C, Pillet C, Martinez A, Prunier C, Barette C, Soleilhac E (2012) Pharmacological inhibition of LIM Kinase stabilizes microtubules and inhibits neoplastic growth. Cancer Res 72:4429–4439
40. Van Aelst L, D'Souza-Schorey C (1997) Rho GTPases and signaling networks. Genes Dev 11(18):2295–2322
41. Fehon RG, McClatchey AI, Bretscher A (2011) Organizing the cell cortex: the role of ERM proteins. Nat Rev Mol Cell Biol 11(4):276–287
42. Sander EE, ten Klooster JP, van Delft S, van der Kammen RA, Collard JG (1999) Rac downregulates Rho activity: reciprocal balance between both GTPases determines cellular morphology and migratory behavior. J Cell Biol 147(5):1009–1022
43. Lammers M, Meyer S, Kuhlmann D, Wittinghofer A (2008) Specificity of interactions between mDia isoforms and Rho proteins. J Biol Chem 283(50):35236–35246
44. Bershadsky AD, Ballestrem C, Carramusa L, Zilberman Y, Gilquin B, Khochbin S, Alexandrova AY, Verkhovsky AB, Shemesh T, Kozlov MM (2006) Assembly and mechanosensors function of focal adhesions: experiments and models. Eur J Cell Biol 85(3–4):165–173
45. Galbraith CG, Yamada KM, Sheetz MP (2002) The relationship between force and focal complex development. J Cell Biol 159(4):695–705
46. Puklin-Faucher E, Sheetz MP (2009) The mechanical integrin cycle. J Cell Sci 122(Pt 2):179–186
47. Sawada Y, Tamada M, Dubin-Thaler BJ, Cherniavskaya O, Sakai R, Tanaka S, Sheetz MP (2006) Force sensing by mechanical extension of the Src family kinase substrate p130Cas. Cell 127(5):1015–1026
48. Barbieri JT, Sun J (2004) *Pseudomonas aeruginosa* ExoS and ExoT. Rev Physiol Biochem Pharmacol 152:79–92
49. Fraylick JE, Rucks EA, Greene DM, Vincent TS, Olson JC (2002) Eukaryotic cell determination of ExoS ADP-ribosyltransferase substrate specificity. Biochem Biophys Res Commun 291(1):91–100
50. Kazmierczak BI, Mostov K, Engel JN (2004) Epithelial cell polarity alters Rho-GTPase responses to *Pseudomonas aeruginosa*. Mol Biol Cell 15(2):411–419
51. Mao Y (2011) FORMIN a link between kinetochores and microtubule ends. Trends Cell Biol 21(11):625–629
52. Mogilner A, Keren K (2009) The shape of motile cells. Curr Biol 19(17):R762–R771
53. Boyer L, Doye A, Rolando M, Flatau G, Munro P, Gounon P, Clement R, Pulcini C, Popoff MR, Mettouchi A, Landraud L, Dussurget O, Lemichez E (2006) Induction of transient macro apertures in endothelial cells through RhoA inhibition by *Staphylococcus aureus* factors. J Cell Biol 173(5):809–819
54. Higgs HN (2001) Actin nucleation: nucleation-promoting factors are not all equal. Curr Biol 11(24):R1009–R1012